研究成果の刊行に関する一覧表

書籍

著者氏名	論文タイトル名	書籍全体の編集者名	書　籍　名	出版社名	出版地	出版年	ページ
宮本将平 土方康基 岡崎利彦 谷憲三朗	樹状細胞療法の現状-当科で実施中の進行固形腫瘍患者に対する強化養子免疫細胞療法臨床研究を中心に-	古山正史	臨床と研究	大道学館出版部	福岡市	2011	42-48

雑誌

発表者氏名	論文タイトル名	発表誌名	巻号	ページ	出版年
Inoue T, Sugiyama D, Kurita R, Oikawa T, Kulkeaw K, Kawano H, Miura Y, Okada M, Suehiro Y, Takahashi A, Marumoto T, Inoue H, Komatsu N, Tani K.	APOA-1 is a novel marker of erythroid cell maturation from hematopoietic stem cells in mice and humans.	Stem Cell Rev	7	43-52	2011
Zhang T, Hamada K, Hyodo M, Itoh H, Tani K, Goda H, Nakashiro K, Hamakawa, H.	Gene therapy for oral squamous cell carcinoma with IAI.3B promoter-driven oncolytic adenovirus -infected carrier cells.	Oncol Rep	25	795-802	2011
Tian Y, Kobayashi S, Ohno N, Isobe M, Tsuda M, Zaike Y, Watanabe N, Tani K, Tojo A, Uchimaru K.	Leukemic T cells are specifically enriched in a unique CD3(dim) CD7(low)subpopulation of CD4(+) T cells in acute-type adult T-cell leukemia.	Cancer Science	102	569-577	2011
Inoue T, Kulkeaw K, Okayama S, Tani K, Sugiyama D	Variation in mesodermal and hematopoietic potential of adult skin-derived induced pluripotent stem cell lines in mice.	Stem Cell Rev	7	958-968	2011
Maeda T, Kurita R, Yokoo T, Tani K, Makino N.	Telomerase inhibition promotes an initial step of cell differentiation of primate embryonic stem cell.	Biochem Biophys Res Commun	407	491-494	2011
Takahashi A, Tokita H, Takahashi K, Takeoka T, Murayama K, Tomotsune D, Ohira M, Iwamatsu A, Ohara K, Yazaki K, Koda T, Nakagawara A, Tani K.	A novel potent tumour promoter aberrantly overexpressed in most human cancers.	Sci Rep	1	1-15	2011

Miyamoto S, Inoue H, Nakamura T, Yamada M, Sakamoto C, Urata Y, Okazaki T, Marumoto T, Takahashi A, Takayama K, Nakanishi Y, Shimizu H, Tani K.	Coxsackievirus B3 Is an oncolytic virus with immunostimulatory properties that is active against lung adenocarcinoma.	Cancer Research	72	2609-2621	2012
Somada S, Muta H, Nakamura K, Sun X, Honda K, Ihara E, Akiho H, Takayanagi R, Yoshikai Y, Podack, ER, Tani K	CD30 Ligand/CD30 interaction is involved in pathogenesis of inflammatory bowel disease.	Dig Dis Sci	—	in press	2012
Dong Y, Kobayashi S, Tian Y, Ozawa M, Hiramoto T, Izawa K, Bai Y, Soda Y, Sasaki E, Itoh T, Maru Y, Oyaizu N, Tojo A, Kai C, Tani K.	Leukemogenic fusion gene (p190 BCR-ABL) transduction into hematopoietic stem/progenitor cells in the common marmoset.	Open J Blood Dis.	—	in press	2012
Zhang T, Hamada K, Hyodo M, Itoh H, Tani K, Goda H, Nakashiro K, Hamakawa H.	Gene therapy for oral squamous cell carcinoma with IAI.3B promoter-driven oncolytic adenovirus-infected carrier cells.	Oncol Rep.	25	795-802	2011
Saito A, Morishita N, Mitsuoka C, Kitajima S, Hamada K, Lee K M, Kawabata M, Fujisawa M, Shirakawa T.	Intravenous injection of irradiated tumor cell vaccine carrying oncolytic adenovirus suppressed the growth of multiple lung tumors in a mouse squamous cell carcinoma model.	J Gene Med.	13	353-361	2011
Hamada K, Yoshihara C, Ito T, Tani K, Tagawa M, Sakuragawa N, Itoh H, Koyama Y.	Antitumor effect of chondroitin sulfate-coated ternary granulocyte macrophage-colony-stimulating factor plasmid complex for ovarian cancer.	J Gene Med.	14	120-127	2012
Yoshihara ., Hamada K, Kuroda M. and Koyama Y.	Oncolytic plasmid: A novel strategy for tumor immuno-gene therapy.	Oncology Letters	3	387-390	2012

Stem Cell Rev and Rep (2011) 7:43–52
DOI 10.1007/s12015-010-9140-7

APOA-1 is a Novel Marker of Erythroid Cell Maturation from Hematopoietic Stem Cells in Mice and Humans

Tomoko Inoue · Daisuke Sugiyama · Ryo Kurita · Tatsuo Oikawa · Kasem Kulkeaw · Hirotaka Kawano · Yoshie Miura · Michiyo Okada · Youko Suehiro · Atsushi Takahashi · Tomotoshi Marumoto · Hiroyuki Inoue · Norio Komatsu · Kenzaburo Tani

Published online: 8 April 2010

Abstract The mechanism that regulates the terminal maturation of hematopoietic stem cells into erythroid cells is poorly understood. Therefore, identifying genes and surface markers that are restricted to specific stages of erythroid maturation will further our understanding of erythropoiesis. To identify genes expressed at discrete stages of erythroid development, we screened for genes that contributed to the proliferation and maturation of erythropoietin (EPO)-dependent UT-7/EPO cells. After transducing erythroid cells with a human fetal liver (FL)-derived lentiviral cDNA library and culturing the cells in the absence of EPO, we identified 17 candidate genes that supported erythroid colony formation. In addition, the mouse homologues of these candidate genes were identified and their expression was examined in E12.5 erythroid populations by qRT-PCR. The expression of candidate erythroid marker was also assessed at the protein level by immunohistochemistry and ELISA. Our study demonstrated that expression of the *Apoa-1* gene, an apolipoprotein family member, significantly increased as hematopoietic

Electronic supplementary material The online version of this article (doi:10.1007/s12015-010-9140-7) contains supplementary material, which is available to authorized users.

T. Inoue · R. Kurita · T. Oikawa · H. Kawano · Y. Miura · M. Okada · Y. Suehiro · A. Takahashi · T. Marumoto · H. Inoue · K. Tani (✉)
Department of Molecular Genetics,
Medical Institute of Bioregulation, Kyushu University,
3-1-1, Maidashi, Higashi-ku,
Fukuoka 812-8582, Japan
e-mail: taniken@bioreg.kyushu-u.ac.jp

T. Inoue
e-mail: yokotomo@bioreg.kyushu-u.ac.jp

R. Kurita
e-mail: k-ryo@brc.riken.jp

T. Oikawa
e-mail: oitatsullo@yahoo.co.jp

H. Kawano
e-mail: kawano@bioreg.kyushu-u.ac.jp

Y. Miura
e-mail: ymiura@bioreg.kyushu-u.ac.jp

M. Okada
e-mail: okadatch@bioreg.kyushu-u.ac.jp

Y. Suehiro
e-mail: suehiro@sentan.med.kyushu-u.ac.jp

A. Takahashi
e-mail: atsushi@sentan.med.kyushu-u.ac.jp

T. Marumoto
e-mail: marumoto@sentan.med.kyushu-u.ac.jp

H. Inoue
e-mail: hinoue@bioreg.kyushu-u.ac.jp

D. Sugiyama
Faculty of Medical Sciences, Department of Hematopoietic Stem Cells, SSP Stem Cell Unit, Kyushu University,
3-1-1, Maidashi, Higashi-ku,
Fukuoka 812-8582, Japan
e-mail: sugiyama@hsc.med.kyushu-u.ac.jp

K. Kulkeaw
Faculty of Medical Sciences, Department of Hematopoietic Stem Cells, SSP Stem Cell Unit, Kyushu University,
3-1-1, Maidashi, Higashi-ku,
Fukuoka 812-8582, Japan
e-mail: kkulkeaw@yahoo.com

N. Komatsu
Department of Transfusion Medicine and Stem Cell Regulation,
Juntendo University School of Medicine,
2-1-1, Hongo, Bunkyo-ku,
Tokyo 113-8431, Japan
e-mail: komatsun@juntendo.ac.jp

stem cells differentiated into mature erythroid cells in the mouse FL. The Apoa-1 protein was more abundant in mature erythroid cells than hematopoietic stem and progenitor cells in the mouse FL by ELISA. Moreover, *APOA-1* gene expression was detected in mature erythroid cells from human peripheral blood. We conclude that APOA-1 is a novel marker of the terminal erythroid maturation of hematopoietic stem cells in both mice and humans.

Keywords APOA-1 · Erythroid cell maturation · Fetal liver erythropoiesis · Library screening · Lentiviral cDNA library

Introduction

Hematopoiesis is the process in which pluripotent hematopoietic stem cells (HSCs) are generated, differentiated into specific progenitors, and ultimately matured into a variety of blood cell types (erythrocytes, megakaryocytes, lymphocytes, neutrophils, and macrophages) [1]. During embryonic development, HSCs emerge in the aorta-gonad-mesonephros (AGM) region and expand first in the fetal liver (FL) and then in the bone marrow (BM) [2–5]. Among these hematopoietic organs, the FL is a site of both HSC expansion and active erythropoiesis [6]. Erythropoiesis is the process by which a vast number of enucleated red blood cells (RBCs) are produced from hematopoietic stem cells (HSC) [7]. However, the molecular mechanisms underlying erythropoiesis have not been fully elucidated, largely because there are only a few molecular markers of terminal erythroid maturation in both mice and humans. To address this issue, we focused on the events that regulate the terminal erythropoiesis of HSCs to mature erythroid cells in order to identify novel markers of mature erythrocytes.

A previous study established a mouse embryonic (ES) cell-derived erythroid progenitor (MEDEP) cell line [8]. Although erythroblasts expressing the erythroid maturation marker Ter119 [9] (a protein that molecularly resembles glycophorin) can be generated from ES/iPS-derived MEDEP cells, most of these cells remained nucleated, indicating that they have failed to complete terminal maturation. Ter119 antigen is currently the only erythroid-specific marker in mice. However, Ter119 is expressed at many maturation stages, from erythroblasts to mature, circulating erythrocytes. Therefore, additional markers for mature erythrocytes are needed. Numerous attempts at generating vast quantities of enucleated erythrocytes have failed to efficiently give rise to fully functional erythrocytes in vitro. This may in part be due to the gaps in our understanding of the mechanisms that regulate erythropoiesis.

The cytokine erythropoietin (EPO) plays important roles in erythropoiesis by regulating erythroid cell differentiation, maturation, proliferation, and survival. Erythroid cells are highly dependent on EPO during early differentiation and maturation but lose this dependency and express lower levels of the erythropoietin receptor (EPOR) as they mature [10]. We hypothesized that EPO-independent signaling plays an important role in the terminal stages of erythropoiesis.

We previously established a system in which specific lentiviral gene transduction induced hematopoiesis from embryonic stem cells of a nonhuman primate common marmoset in the absence of bone marrow stromal cells [11]. In addition, we constructed a high-performance human fetal liver (FL)-derived cDNA lentiviral library as a tool to facilitate the discovery of novel genes that are involved in the expansion of HSCs, erythropoiesis and/or liver development [12]. During embryogenesis, the FL is the major site of hematopoiesis, particularly erythropoiesis. Therefore, the FL-derived cDNA lentiviral library that we constructed contains many genes that are involved in the differentiation and maturation of these lineages. The goal of this study was to identify novel genes that are involved in or expressed during EPO-independent terminal erythroid maturation. We identified APOA-1 as a novel marker of the maturation of hematopoietic stem cells into mature erythroid cells.

Materials and Methods

Cells

UT-7/EPO cells [13] (kindly provided by Dr. Komatsu) are an EPO-dependent cell line that was established from the bone marrow of a patient with acute megakaryoblastic leukemia. This cell line was cultured in Iscove's modified Dulbecco's medium (IMDM) supplemented with 10% fetal bovine serum (FBS) and 1 U/mL human recombinant EPO (R&D Systems, Minneapolis, MN) at 37°C in 5% CO_2.

Lentivirus Production

The previously generated human fetal liver-derived Entry cDNA library [12] was used in this study. Briefly, 34 μg ($1–2\times10^5$ cDNA clones) of the library was mixed with 20 μg of pCAG-HIVg/p and 20 μg of pCMV-VSVG-RSV-Rev as the packaging plasmids in 3.5 ml of FBS-free DMEM, and then 370 μl of 1 mg/ml polyethylenimine (PEI) was added to the mixture. After a 30-min incubation, the DNA/PEI complexes were dropped onto semi-

confluent 293 T cells in a T175 flask containing Opti-MEM medium and then incubated for 3 h. Next, these cells were cultured in DMEM containing 10% FBS. Virus-containing supernatants were harvested 4 days post transduction and concentrated by centrifugation (9,000 rpm, 6–8 h, 4°C). The virus pellet was resuspended in 1 ml of IMDM and used for overnight transduction of UT-7/EPO cells.

Transduction of the Lentiviral Library into UT-7/EPO Cells

UT-7/EPO cells were transduced with the viral cDNA library and cultured in methylcellulose semi-solid medium containing IMDM, 10% FBS, and P/S without EPO for one month. After this period, several colonies were harvested, and genomic DNA was isolated from each colony using the QIAamp DNA Micro Kit (Qiagen, Valencia, CA).

Genomic PCR and Sequence Analysis

The integrated cDNAs were PCR amplified using a forward primer (5′-TTCAGGTGTCGTGAACACGCTACCG-3′) and reverse primer (5′-CCTCGATGTTAACTCTAGAG GATCC-3′). The Expand Long Template PCR System (Roche, Basel, Switzerland) was used following the manufacturer's protocol. cDNAs that were cloned into the CSII-CMV-RfA vector were sequenced with the forward (5′-CAAGCCTCAGACAGTGG-3′) and reverse (5′-AGCG TATCCACATAGCG-3′) primers using a Big-Dye Terminator v3.1 Cycle sequencing kit (Applied Biosystems, Foster City, CA) and an ABI PRISM 3100 Genetic Analyzer (Applied Biosystems). The sequences were compared with the DNA database from the DNA Data Bank of Japan using BLAST.

Cell Culture and Sorting

The EPO-dependent UT-7/EPO cell line was established and cultured as previously reported [13]. C57BL6J mice and ICR mice were purchased from Nihon SLC. Twelve o'clock noon was considered to be 0.5 day postcoitum (dpc) for plugged mice. Fetal liver (FL) cells from a 12.5 dpc embryo were filtered through a 40 μM nylon mesh and washed with PBS. The cells were stained with a FITC-conjugated anti-mouse CD71 Ab (BD Biosciences), PE-conjugated anti-mouse Sca-1 Ab (BD Biosciences), APC-conjugated anti-mouse c-Kit Ab (BD Biosciences), PE-Cy7-conjugated anti-mouse CD45 Ab (eBioscience) and APC-Cy7-conjugated anti-mouse Ter119 Ab (eBioscience). The cells were sorted using a FACS Aria cell sorter (BDIS), and the data files were analyzed using FlowJo software (Tree Star, Inc.).

Human peripheral blood (PB) was obtained from healthy volunteers. The PB was stained with a FITC-conjugated anti-human CD45 Ab (eBioscience), PE-conjugated anti-GPA antibody (eBioscience) and APC-conjugated anti-human CD41 antibody (BD Bioscience). The cells were sorted using a FACS Aria cell sorter (BDIS), and the data files were analyzed using FlowJo software (Tree Star, Inc.).

All animal studies were approved by the Committee on Ethics in Animal Experiments of Kyushu University, and the human studies were approved by the Committee on Ethics in Human clinical samples of Kyushu University. All of these studies were performed following the guidelines of Kyushu University.

RNA Extraction and Real-time RT-PCR

Total RNA was isolated from FL cells of ICR embryos at 12.5 dpc or whole embryos at 10.5 dpc using the RNAqueous-4PCR kit (Ambion). Total RNA from human peripheral blood was isolated with the RiboPure Kit (Ambion). A high-capacity cDNA Archive kit (Applied Biosystems) was used to synthesize cDNA from RNA. The mRNA levels of various genes were analyzed by qRT-PCR using SYBR Green and gene-specific primers with the StepOnePlus real-time PCR system (Applied Biosystems). The mRNA level of each target gene was normalized to β-actin as an internal control.

Immunohistochemistry

Ter119-positive cells from 12.5 dpc FL cells were isolated by flow cytometry as described above. Cells were cytospun onto glass slides and air-dried. The cells were fixed in 1% PFA at room temperature (RT) for 10 min. Nonspecific binding was blocked by incubating the cells at RT for 30 min in a blocking solution containing 1% BSA and 0.05% Triton X-100 in PBS. The following antibodies were diluted in the blocking solution: rabbit anti-Apoa-1 (1:50, Santa Cruz Biotechnologies, Inc.). A donkey anti-rabbit IgG (H+L)-Alexa555 (1:250, Invitrogen) was used as secondary antibody and TOTO-3 (1:1500, Invitrogen) was added as a nuclear stain. Coverslips were mounted with fluorescent mounting medium (Dako), and the slides were examined using a confocal microscope (Olympus).

ELISA

c-Kit-positive cells and Ter119-positive cells were isolated by flow cytometry as described above. Proteins were extracted from the sorted cells using the Qproteome Mammalian Protein Preparation kit (Qiagen). To detect the Apoa-1 protein, a goat anti-Apoa-1 (0.8 μg/ml,

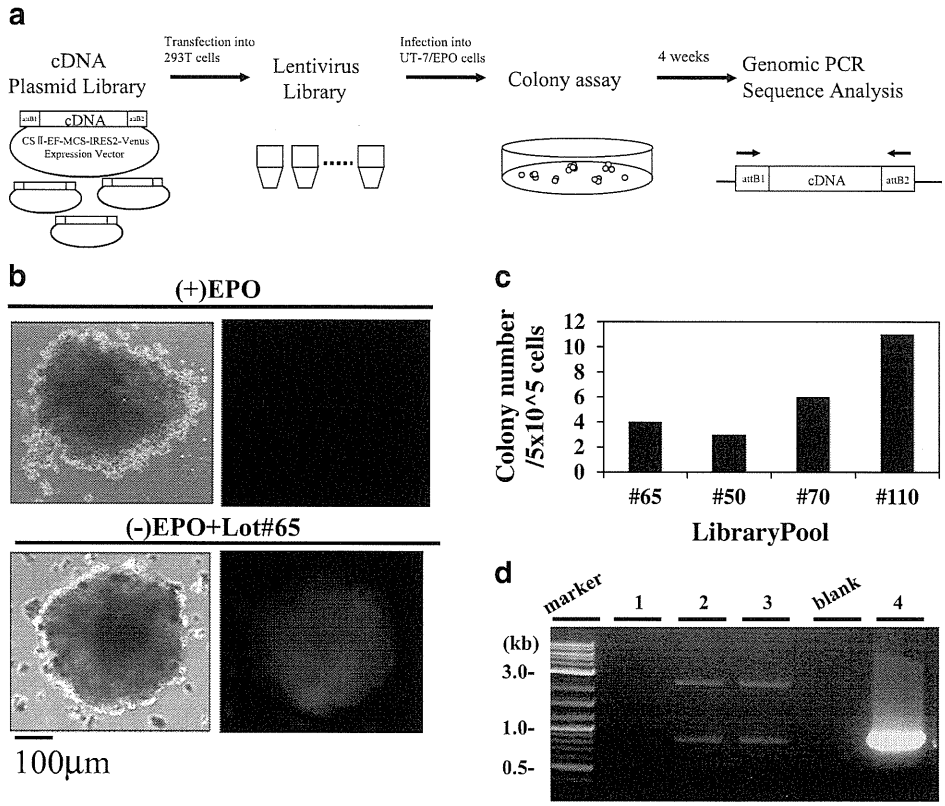

Fig. 1 Lentiviral human FL cDNA library screening in UT-7/EPO cells. **a** Strategy for identifying candidate EPO-independent regulators of erythropoiesis. Four pools (#65, #50, #70 and #110) of human FL-derived cDNA library were transfected into 293 T cells with helper plasmids to generate the lentiviral library. UT-7/EPO cells were transduced with these lentiviral library pools and then cultured in semisolid, EPO-deficient media for four weeks to positively select for clones that were able to form EPO-independent erythroid colonies. Finally, the cDNAs of the positive clones were sequenced to identify the transduced genes. **b** Erythroid colony assay. UT-7/EPO cells were transduced with the lentiviral pools (#65, #50, #70 and #110) and then transferred to semi-solid culture media. A representative colony derived from cells transduced with pool #65 is shown (Scale bar= 200 μm). A non-transduced colony was negative for Venus, while the lentiviral library-transduced colony was positive for Venus. **c** Colony number. A total of 22 colonies were obtained from UT-7/EPO cells that had been transduced with four lentiviral library pools and then analyzed by the colony formation assay. **d** Genomic PCR analysis. The inserted candidate genes were examined by genomic PCR using lentivirus insertion-specific primers. Lane 1: Untransduced UT-7/EPO cells (negative control), Lanes 2, 3: A colony derived from UT-7/EPO cells that had been transduced with lentiviral pool #65, Lane 4: GFP-transduced UT-7/EPO cells (positive control)

Rockland Immunochemicals) was used as a capture antibody, a rabbit anti-Apoa-1 (1:100, Santa Cruz Biotechnologies, Inc.,) was used as a detection antibody (primary antibody), and an anti-rabbit IgG-HRP (1:5000, Millipore) was used as the secondary antibody. Each antibody was captured onto 96-well immunoplates (Nunc) at 4°C for 16 h. Nonspecific binding was blocked by incubating the plate with 1% BSA/PBS for 2 h at RT. After the extracted proteins were added to the plate for 2 h at RT, the primary antibody was added for 1 h at RT, followed by the secondary antibody for 30 min at RT. The tetramethylbenzidine substrate was added to the wells for 30 min at RT, followed by a Stop Solution (R&D). The O.D. at 450 nm was measured using a Thermo Multiskan EX plate reader.

Results

Screening for Genes that Replace EPO/EPOR Signaling in UT-7/EPO Cells Using a Human FL Lentiviral Library

To identify novel genes that regulate erythroid cell maturation, we designed a strategy that monitored the ability of the EPO-dependent cell line, UT-7/EPO, to form erythropoietin (EPO)-independent colonies. Recently, we constructed a lentiviral human fetal liver (FL) cDNA library to search for novel genes that regulate hematopoiesis, including erythropoiesis [14]. Lentiviral cDNA library pools, which contained $1.32–1.98 \times 10^5$ cfu (colony forming units) per pool [14], were examined in this screen. We used the UT-7/EPO cell line, which is dependent upon EPO [13].

Table 1 Genes transduced in lentiviral-transduced erythroid colonies arising in the absence of Epo

Lentivirus pool #	Gene symbol	Discription
65	Angiotensinogen	AGT
	Estrogen receptor binding site associated antigen 9	EBAG9
50	B-cell CLL/lymphoma 2-like 1	BCL2-like 1
	Apolipoprotein A-1	APOA-1
70	ferritin heavy subunit	FHS
	3-phosphoinositide dependent protein kinase-1	PDPK1
	abl interactor 2	ABI-2
	Fibrinogen like 1	FGL1
	Apolipoprotein E	APOE
	Interferon induced transmembrane protein 2	1-8D
110	Asialoglycoprotein receptor 2	ASGR2
	Ferritin light chain	FLC
	Solute carrier family 27 (fatty acid transporter)	SLC27A2
	Ribosomal protein L10	RPL10
	Collagen type XVIII alpha 1	COL18A1
	Apolipoprotein J	APOJ
	Group-specific component	GC

When UT-7/EPO cells are transduced with genes in this lentiviral library that can functionally replace EPO/EPOR signaling, expression of these genes will result in colony formation in the absence of EPO (Fig. 1a). 293 T cells were transfected with four different lentiviral cDNA pools (#65, #50, #70 and #110). Subsequently, UT-7/EPO cells were transduced with these four different lentivirus library pools and cultured for four weeks in semi-solid media in the absence of EPO. Clones that acquired the ability to proliferate in the absence of EPO were identified and analyzed. Lentiviral-transduced cells were identified by Venus fluorescence that was encoded by the lentiviral vector. UT-7/EPO cells that were cultured in the absence of EPO failed to generate colonies, whereas these cells generated equal numbers of colonies when cultured in semi-solid media containing EPO (data not shown). When UT-7/EPO cells that had been transduced with the lentiviral library (6×10^5 cDNAs) were cultured in the absence of EPO, 22 EPO-independent colonies formed (Fig. 1b–c).

Next, to identify the cDNAs responsible for this EPO-independent proliferation, genomic DNA was isolated from each colony, and the integrated cDNAs were PCR amplified using lentivirus-specific primers (Fig. 1d). Agarose gel electrophoresis of the PCR products for each colony showed multiple bands of different sizes (Fig. 1d, lanes 2 and 3). This amplification was specific because untransduced UT-7/EPO cells did not yield any PCR products (lane 1), and a PCR product of the expected size was amplified from UT-7/EPO cells transduced with a lentivirus encoding green fluorescent protein (GFP) (lane 4).

Candidate Genes Identified from UT-7/EPO Cells Transduced with Human FL Lentiviral cDNA Library

The PCR products from the first round of screening were sequenced to identify the candidate genes that were expressed during erythropoiesis. Each pool contained a different number of inserted genes (Table 1). From the first screening, the following genes were identified as candidates that contributed to the growth of EPO-independent colonies; *FHS* and *FLC* encoding iron-binding proteins; the vitamin D-binding protein *GC*; the plasma protein receptor *ASGR2*; the vasoregulator *AGT*; estrogen-responsive protein *EBAG9*; the collagen *COL18A1*; the ribosomal protein *RPL10*; the kinase *PDPK1*; *ABI-2*, a kinase-binding protein; *APOA-1*, *APOE, APOJ* and *SLC27A2,* all of which encode lipid metabolism-related proteins; the anti-apoptotic protein *BCL2-like1*; and *1-8D,* encoding a protein of unknown function.

Among the integrated genes, some (*AGT*, *FHS*, *1-8D*, *FLC* and *GC*) were inserted into the host genome as a full-length coding sequence (CDS). As a result, these genes produced functional proteins that could be expressed in UT-7/EPO cells and lead to colony formation in the absence of EPO. Other genes (*BCL2-like1*, *APOA-1*, *PDPK1*, *FGL1*, *APOE*, *SLC27A2* and *COL18A1*) were inserted as a partial CDS that lacked the 5′ first start codons but contained 3′ stop codons, indicating that these genes were translated from a secondary start codon to the stop codon to yield partial proteins. As a result, functional proteins may be expressed in UT-7/EPO cells, leading to colony formation in the absence of EPO. The remaining inserted genes (*EBAG9*, *ABI-2*, *ASGR2* and *APOJ*) consisted of only a

Table 2 Gene specific primers for candidate genes in mice

Agt	5′	AGTGGGAGAGGTTCTCAATAGCA
	3′	GACGTGGTCGGCTGTTCCT
Ebag9	5′	GCAGCTACACAAGACATGCCTTT
	3′	TCCCACGCATTGCTATTTTCT
Bcl2-like1	5′	GGCTGGGACACTTTTGTGGAT
	3′	AAGCGCTCCTGGCCTTTC
Apoa-1	5′	GACAGCGGCAGAGACTATGTGT
	3′	AGGAGATTCAGGTTCAGCTGTTG
Fhs	5′	GCATGCCGAGAAACTGATGA
	3′	TCACGGTCTGGTTTCTTTATATCCT
Pdpk1	5′	TTCTTGGCGAGGGCTCTTT
	3′	CATATTCTCTGGAAGTGGCCAGTT
Abi-2	5′	GCGGGTGGCCGACTACT
	3′	TCTTCTAGGGCTCGCTGCTT
Apoe	5′	AGCTGCAGAGCTCCCAAGTC
	3′	TTACTTCCGTCATAGTGTCCTCCAT
1-8d	5′	CCTGGGCTTCGTTGCCTAT
	3′	CACATCGCCCACCATCTTC
Asgr2	5′	GGAGGAGAAGCAGCAACAGCTA
	3′	TGGGAAGTGCTTCAGGTGAAA
Flc	5′	CGGGCCTCCTACACCTACCT
	3′	GCCACGTCATCCCGATCA
Slc27a2	5′	CAACACACCGCAGAAACCAA
	3′	CCATTTCCCAGGGCTTTTTT
Rpl10	5′	TTCCATGTCATCCGTATCAACAA
	3′	CCCTGTCTGGAGCCTGTCA
Col18a1	5′	GCAGAGCCAGAGAATGTTGCT
	3′	CCCGACGTGAGGGTCATC
Apoj	5′	GGTCGGCCAGCAGCTAGAG
	3′	CGCCGTTCATCCAGAAGTAGA
Gc	5′	GGATCCTGCTGTACTTCTGCAA
	3′	TGCTTCATCTGGAGTCTCTCCTT

partial CDS without an open reading frame (ORF). These genes were translated from the shifted reading frame of the original mRNA and produced proteins of uncertain function. However, these genes resulted in UT-7/EPO colony formation in the absence of EPO. All of the 17 candidate cDNAs with full-length, partial or matched ORFs or partial but non-matched ORFs were examined in a secondary screen to identify specific genes that were involved in terminal erythroid maturation.

Expression of EPO-independent Growth-inducing Genes in Mouse FL Erythroid Populations

To determine which candidate genes obtained from first screen are critical for primary erythroid cell maturation, we performed a second screen to analyze gene expression during erythroid development. We used mouse fetuses for the second screen since mouse fetal samples are easier to obtain and use than human samples. The mouse homologues of these candidate genes were identified and the expression of the candidate genes was analyzed by RT-PCR using gene-specific primers (Table 2).

First, gene expression was assessed in samples from E10.5 whole embryos (WE) and E12.5 FL. All candidate genes were expressed in E12.5 FL with the exception of *Asgr-2,* which was eliminated as a gene of interest (Fig. 2). *Ebag9* and *Col18a1* expression was lower in the FL than in the whole E10.5 embryos, while *Fhs* and *Gc* had the opposite expression pattern with higher expression in the FL samples.

Next, we analyzed candidate gene expression in a series of FL-derived hematopoietic populations ranging from uncommitted hematopoietic stem cells (HSCs) to mature erythrocytes as determined by the expression of the surface markers CD45, Sca-1, c-Kit, CD71 and Ter119 (Fig. 3a). The following criteria were used to identify each hematopoietic population: (1) CD45+/Sca-1+/c-Kit+ cells represent HSCs; (2) c-Kit+ (Sca-1-/c-Kit+/CD71-/Ter119-) cells are BFU-E; (3) c-Kit+/CD71+ (Sca-1-/c-Kit+/CD71+/Ter119-) cells are committed erythroid progenitor cells or CFU-E; (4) CD71+/Ter119+ (Sca-1-/c-Kit-/CD71+/Ter119+) cells are proerythroblasts; and (5) Ter119+ (Sca-1-/c-Kit-/CD71-/Ter119+) cells represent mature erythroblasts and erythrocytes (Fig. 3a) [14, 15].

The mRNA expression of some candidate genes (*Abi-2*, *Slc27a2*) was higher in HSCs and gradually decreased throughout erythroid cell maturation (Fig. 3b). The expression of other candidate genes (*Pdpk1*, *Fhs*, *Flc*, *Rpl10*, *Ebag9* and *Apoe*) increased from HSCs to erythroblasts and then gradually decreased from erythroblasts to mature erythrocytes. *Bcl2l1* expression was low in HSCs and gradually increased. *Apoa-1* was highly expressed in

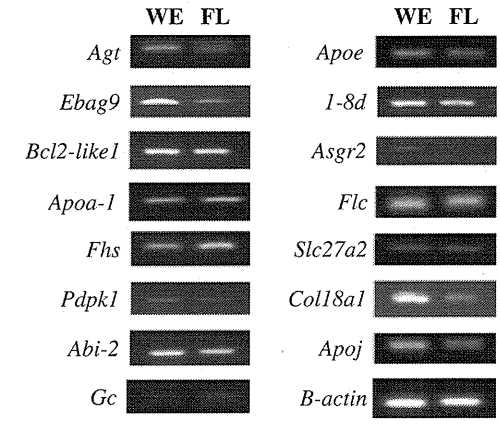

Fig. 2 Expression of candidate erythroid genes in developing mouse embryos. RT-PCR analyses of candidate genes in mouse embryos. We used RT-PCR to examine the expression patterns of the mouse homologues of each candidate gene in 10.5 dpc whole embryos (WE) and 12.5 dpc FL in ICR mouse embryos

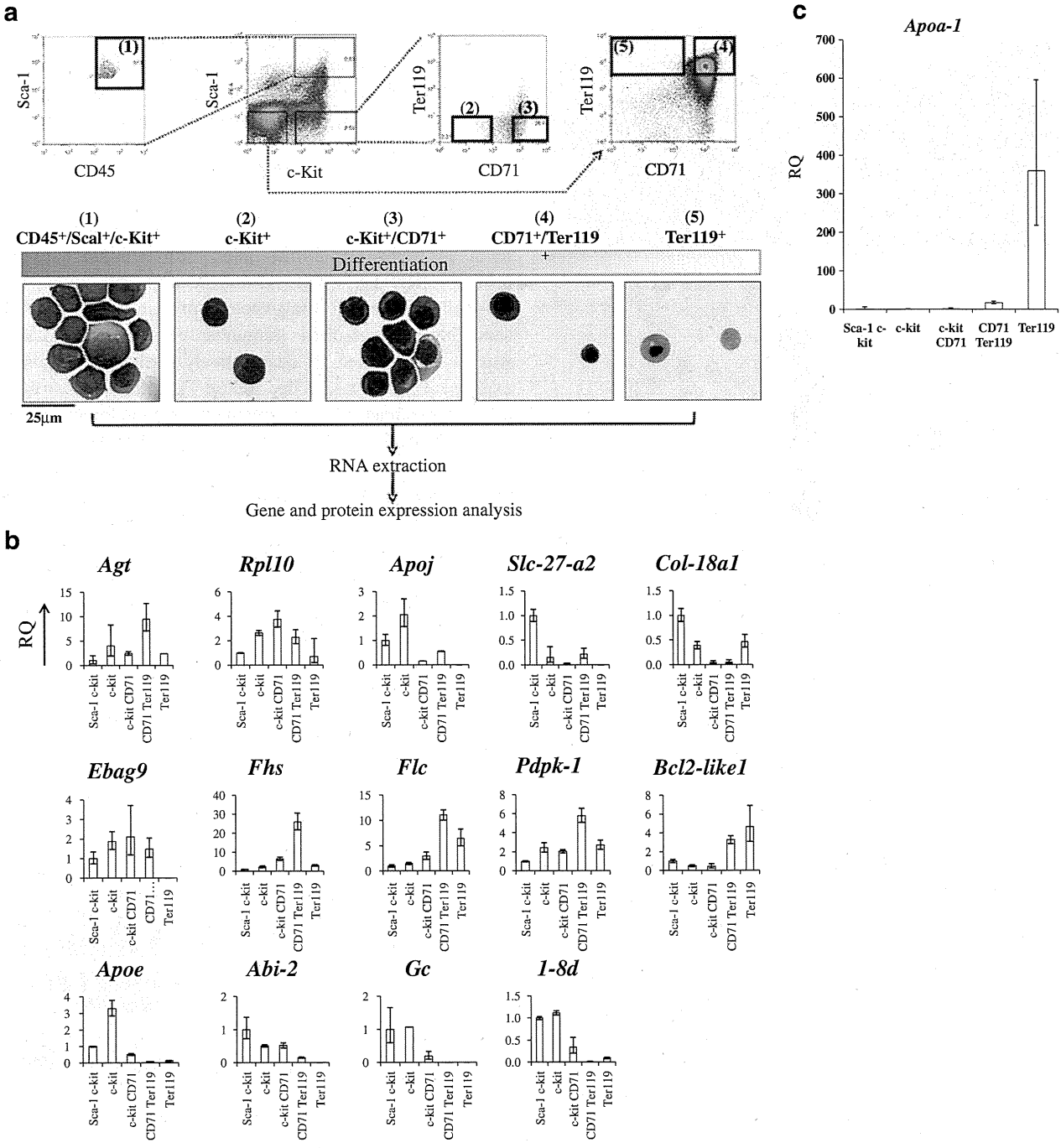

Fig. 3 Isolation of maturing erythroid populations from mouse FL cells. **a** Hematopoietic stem cells and maturing erythroid populations were isolated from 12.5 dpc mouse FL based on the expression of the surface markers CD45 (common leukocyte antigen), Sca-1 (stem cell antigen-1), c-Kit (stem cell factor receptor), CD71 (transferrin receptor) and Ter119 (Glycophorin A-associated antigen). The cytospins of each cellular fraction were prepared for May-Grunwald-Giemsa staining. As erythroid cells mature, the cell size decreased and finally the erythrocytes were enucleated. **b** mRNA expression patterns of candidate genes during erythroid cell maturation. The mRNA levels of candidate genes in maturing erythroid populations were analyzed by qRT-PCR. Total RNA was isolated from FL cells of 12.5 dpc embryos (Bars represent the means ± SD). The horizontal axes indicate the HSC fraction and the erythroid cell stage. Erythroid cell development proceeds from left to right. The vertical axes indicate the relative quantitation (RQ) of mRNA expression with the Sca-1^+/c-Kit^+ cell fraction set at an RQ value of 1. **c** The expression of mouse *Apoa-1* was significantly increased in the terminal maturation stages ($Ter119^+$ cell fraction) of cells obtained from 12.5 dpc FL

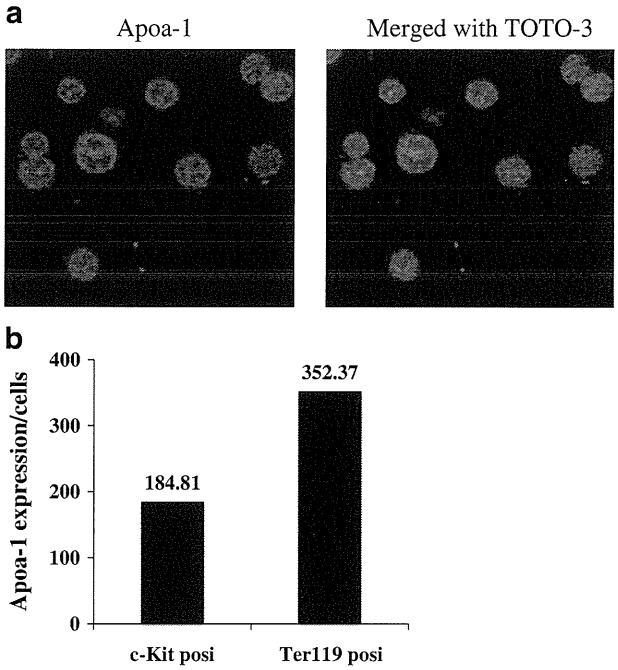

Fig. 4 Apoa-1 protein expression in mouse FL cells. **a** Immunohistochemistry. Ter119-positive cells from 12.5 dpc FL cells were cytospun and stained with an anti-mouse Apoa-1 antibody. Apoa-1-positive cells (*red*) were observed in 12.5 dpc FL cells. Nuclei were stained with TOTO3 (*blue*). **b** ELISA. c-Kit-positive cells and Ter119-positive cells from 12.5 dpc FL cells were sorted. Protein was extracted from each fraction and then analyzed by a sandwich ELISA. The expression levels of the mouse Apoa-1 proteins are shown for each fraction

Ter119-positive mature erythrocytes (Fig. 3c). The mRNA levels of *Apoa-1* increased approximately 350-fold, respectively, in the Ter119-positive cell population compared to the HSC population, suggesting that both of these genes are involved in the terminal maturation of erythroid cells.

Expression of the Apoa-1 Protein in Mouse FL Cells

To determine whether Apoa-1 is expressed at the protein level in mouse erythroid cells, immunohistochemical analyses were performed. Ter119-positive cells in mouse FL cells expressed the Apoa-1 protein (Fig. 4a). A sandwich enzyme-liked immunosorbent assay (ELISA) was also performed to quantitatively analyze the protein expression level in 12.5 dpc mouse FL cells. Because it is difficult to extract sufficient amounts of protein for an ELISA from individually fractionated cells in the populations shown in Fig. 3a, we compared the following two groups to analyze protein expression: c-Kit-positive cells, namely ((1)+(2)+(3) in Fig. 3) and Ter119-positive cells or ((4)+(5) in Fig. 3). As shown in Fig. 4b, Apoa-1 protein expression was approximately two-fold higher in Ter119-positive cells than c-Kit-positive cells, indicating that Apoa-1 expression correlates with terminal erythroid maturation at the protein level.

APOA-1 Expression in Human Peripheral Blood

To determine whether APOA-1 is useful as a terminal erythroid marker in human samples, we examined mRNA

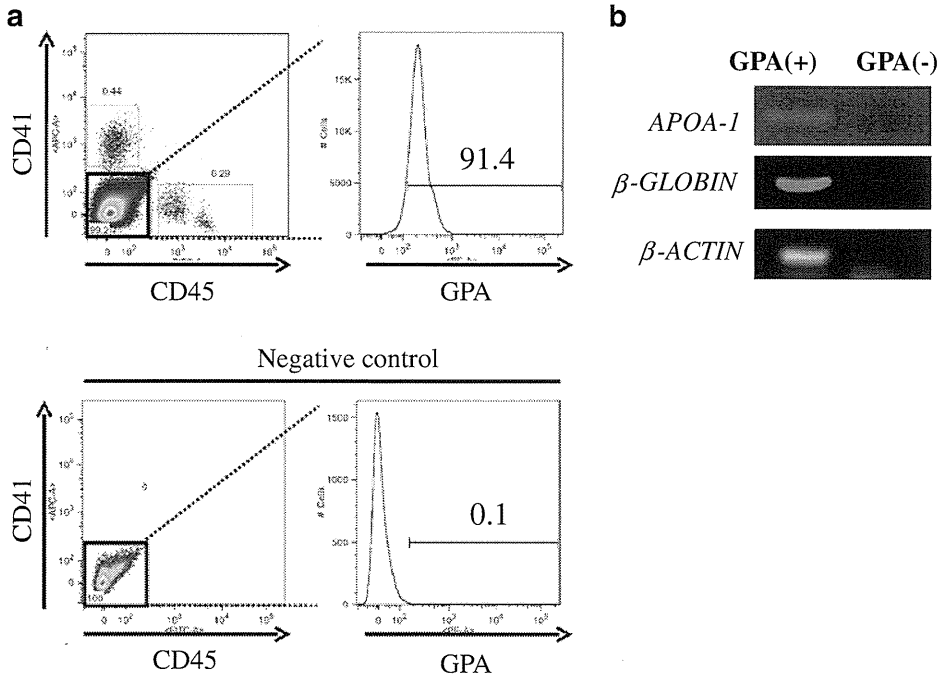

Fig. 5 *APOA-1* gene expression in human peripheral blood. **a** Erythrocytes and reticulocytes were isolated from human peripheral blood based on the expression of surface markers CD41 (integrin IIb), CD45 (common leukocyte antigen) and GPA (glycophorin A). **b** RT-PCR was performed to assess expression of human *APOA-1*. Human *β-GLOBIN* expression was analyzed to confirm that erythrocytes and reticulocytes had been isolated by flowcytometry. *APOA-1* was expressed in human peripheral blood

expression in human peripheral blood (PB) erythrocytes and reticulocytes. Erythrocytes and reticulocytes were isolated from peripheral blood by flow cytometry based on the expression of the cell surface markers glycophorin A (GPA), CD41 and CD45. In the PB, 91.4% of the CD41-/CD45-cells were positive for GPA (Fig. 5a). Reverse transcriptase PCR (RT-PCR) analysis showed that *β-GLOBIN* was expressed in GPA-positive cells, indicating that erythrocyte and reticulocyte mRNA was successfully extracted from the PB (Fig. 5b). Furthermore, *APOA-1* mRNA was expressed in the same fraction, demonstrating that this molecules can be used as a potential marker for terminal erythroid maturation in humans as well as mice.

Discussion

The goal of this study was to identify novel genes that are expressed during the terminal, EPO-independent maturation of erythroid cells. A two-step approach consisting of a lentiviral human FL cDNA library screen followed by an analysis of the gene expression patterns during erythropoiesis was performed to efficiently identify target genes.

This strategy had two clear advantages. First, it is important to establish a screening system that can detect erythropoiesis-related genes in an EPO-independent manner. A human FL cDNA library can be screened to identify novel genes. In this study, UT-7/EPO cells were transduced with a FL cDNA expression lentiviral library to detect genes that generate erythroid colonies in semi-solid medium in the absence of the EPO signaling pathway. Second, this screen could examine the effects of a large number (6×10^5) of genes on erythroid maturation. As humans are estimated to have approximately $2–3\times10^4$ genes, our screening encompassed a sufficient number of human cDNAs.

BCL2-like1 (BCL2L1) was one of the candidate genes identified in the first screen. *BCL2L1* encodes an anti-apoptotic protein that plays an important role in erythropoiesis in the absence of EPO [16]. Therefore, the results of our first screen strongly indicated that this system could be used to identify EPO-independent erythropoiesis-related genes. Other candidate genes included *FHS* and *FLC*, which encode iron-binding proteins, and *APOE, APOA-1*, *APOJ* and *SLC27A2,* which encode lipid metabolism-related proteins. Both iron and lipid metabolism are important cellular processes that regulate erythroid maturation [17–19]. We also identified a number of genes that were not previously implicated in erythropoiesis, including a vitamin D-binding protein (*GC)*, vasoregulator (*AGT)*, estrogen-responsive gene (*EBAG9*), collagen type 18 *(COL18A1)*, ribosomal protein (*RPL10*) and several kinase-related proteins (*PDPK1* and *ABI-2*).

We also specifically identified a gene that was upregulated in the terminal stages of erythrocyte maturation. The identification of this gene is significant because very few molecular markers can be used to examine this stage of erythropoiesis. The candidate gene, *APOA-1*, was particularly interesting. APOA-1 is a major protein component of high-density lipoprotein (HDL) in the plasma and promotes the efflux of cholesterol from the tissues to the liver for excretion [20]. APOA-1 is a cofactor for lecithin cholesterol acyltransferase (LCAT), which is responsible for the formation of most plasma cholesteryl esters.

APOA-1 interacts with the ATP-binding cassette transporter ABCA1 (member 1 of human transporter sub-family ABCA) [21]. A recent report demonstrated that the APOA-1/ABCA1 pathway functions as an anti-inflammatory receptor by activating Janus Kinase 2 (JAK2)/Signal Transducers and Activation of Transcription3 (STAT3) in macrophages [22]. JAK2/STAT3 and/or JAK2/STAT5 are central signal pathways in erythroid cells [23]. Therefore, APOA-1/ABCA1 may activate the JAK2/STAT3 and/or JAK2/STAT5 pathway during the terminal maturation of erythroid cells.

It is intriguing to note that defects in APOA-1 are associated with low HDL levels observed in HDL deficiency type 1, which includes analphalipoproteinemia or Tangier disease. In Tangier disease patients, APOA-1 fails to associate with HDL. This inability to bind HDL is likely due to the faulty conversion of pro-APOA-1 molecules into mature chains, either due to a defect in the converting enzyme or a specific structural defect [24–26]. Furthermore, red blood cells in patients with Tangier disease have stomatocytosis and hemolytic anemia [27]. Moreover, patients with beta-thalassemia major as well as sickle cell disease have lower levels of APOA-1 in their plasma than healthy controls [28]. This abnormal erythrocyte morphology could be partially explained by a recent report by Holm TM et al., which showed that knockout mice with defects in the high-density lipoprotein receptor SR-BI have abnormal erythrocyte morphology. On the other hand, the fractional catabolic rate (FCR) for APOA-1 was significantly increased in patients with myeloproliferative disorders, including polycythemia vera, compared with healthy controls [29]. Therefore, accelerated red blood cell production could be also supported by increased APOA-1 catabolism. Further studies including both in vitro and/or in vivo analyses of APOA-1 knockouts are necessary to demonstrate the direct importance of APOA-1 in the maturation of red blood cells.

This study is the first to report that APOA-1 is a novel molecular marker for terminal erythroid maturation from HSC. In combination with Ter119 antigen or glycophorin A antigen, this molecule can potentially be used to identify mature erythrocytes in in vitro cultured erythroid cell

sources such as ES or iPS cells. It will be necessary to further investigate whether APOA-1 plays pivotal roles in erythroid cell maturation and is a useful maturation marker.

Acknowledgements The authors would like to thank Chiyo Mizuochi, Yuka Horio, Tatsuya Sasaki and Michiko Ushijima at Kyushu University for excellent technical assistance. This work was supported by a grant from the Project for Realization of Regenerative Medicine from the Ministry of Education, Culture, Sports, Science and Technology and by a grant from the BASIS project from the Ministry of Education, Culture, Sports, Science and Technology. T. Inoue is supported by research fellowships from the Japan Society for the Promotion of Science for Young Scientists.

Disclosures The authors indicate no potential conflicts of interest.

References

1. Weissman, I. L. (2000). Stem cells: units of development, units of regeneration, and units in evolution. *Cell, 100*, 157–168.
2. Mikkola, H. K., & Orkin, S. H. (2006). The journey of developing hematopoietic stem cells. *Development, 133*, 3733–3744.
3. Medvinsky, A., & Dzierzak, E. (1996). Definitive hematopoiesis is autonomously initiated by the AGM region. *Cell, 86*, 897–906.
4. Sugiyama, D., & Tsuji, K. (2006). Definitive hematopoiesis from endothelial cells in the mouse embryo; a simple guide. *Trends in Cardiovascular Medicine, 16*, 45–49.
5. Ema, H., & Nakauchi, H. (2000). Expansion of hematopoietic stem cells in the developing liver of a mouse embryo. *Blood, 95*, 2284–2288.
6. Palis, J. (2008). Ontogeny of erythropoiesis. *Current Opinion in Hematology, 15*, 155–161.
7. McGrath, K., & Palis, J. (2008). Ontogeny of erythropoiesis in the mammalian embryo. *Current Topics in Developmental Biology, 82*, 1–22.
8. Hiroyama, T., Miharada, K., Sudo, K., Danjo, I., Aoki, N., & Nakamura, Y. (2008). Establishment of mouse embryonic stem cell-derived erythroid progenitor cell lines able to produce functional red blood cells. *PLos One, 3*, e1544.
9. Kina, T., Ikuta, K., Takayama, E., et al. (2000). The monoclonal antibody TER-119 recognizes a molecule associated with glycophorin A and specifically marks the late stages of murine erythroid lineage. *British Journal Haematology, 109*, 280–287.
10. Zhang, J., Socolovsky, M., Gross, A. W., & Lodish, H. F. (2003). Role of Ras signaling in erythroid differentiation of mouse fetal liver cells: functional analysis by a flow cytometry-based novel culture system. *Blood, 102*, 3938–3946.
11. Kurita, R., Sasaki, E., Yokoo, T., et al. (2006). Tal1/Scl gene transduction using a lentiviral vector stimulates highly efficient hematopoietic cell differentiation from common marmoset (Callithrix jacchus) embryonic stem cells. *Stem Cells, 24*, 2014–2022.
12. Kurita, R., Oikawa, T., Okada, M., et al. (2008). Construction of a high-performance human fetal liver-derived lentiviral cDNA library. *Molecular and Cellular Biochemistry, 319*, 181–187.
13. Komatsu, N., Yamamoto, M., Fujita, H., et al. (1993). Establishment and characterization of an erythropoietin-dependent subline, UT-7/Epo, derived from human leukemia cell line, UT-7. *Blood, 82*, 456–464.
14. Suzuki, N., Suwabe, N., Ohneda, O., et al. (2003). Identification and characterization of 2 types of erythroid progenitors that express GATA-1 at distinct levels. *Blood, 102*, 3575–3583.
15. Walkley, C. R., & Orkin, S. H. (2006). Rb is dispensable for self-renewal and multilineage differentiation of adult hematopoietic stem cells. *Proceedings of the National Academy of Sciences of the United States of America, 103*, 9057–9062.
16. Dolznig, H., Habermann, B., Stangl, K., et al. (2002). Apoptosis protection by the Epo target Bcl-X(L) allows factor-independent differentiation of primary erythroblasts. *Current Biology, 12*, 1076–1085.
17. Gelvan, D., Fibach, E., Meyron-Holtz, E. G., & Konijn, A. M. (1996). Ferritin uptake by human erythroid precursors is a regulated iron uptake pathway. *Blood, 88*, 3200–3207.
18. Meyron-Holtz, E. G., Vaisman, B., Cabantchik, Z. I., et al. (1999). Regulation of intracellular iron metabolism in human erythroid precursors by internalized extracellular ferritin. *Blood, 94*, 3205–3211.
19. Holm, T. M., Braun, A., Trigatti, B. L., et al. (2002). Failure of red blood cell maturation in mice with defects in the high-density lipoprotein receptor SR-BI. *Blood, 99*, 1817–1824.
20. Breslow, J. L., Ross, D., McPherson, J., et al. (1982). Isolation and characterization of cDNA clones for human apolipoprotein A-I. *Proceedings of the National Academy of Sciences of the United States of America, 79*, 6861–6865.
21. Fitzgerald, M. L., Morris, A. L., Rhee, J. S., Andersson, L. P., Mendez, A. J., & Freeman, M. W. (2002). Naturally occurring mutations in the largest extracellular loops of ABCA1 can disrupt its direct interaction with apolipoprotein A-I. *Journal of Biological Chemistry, 277*, 33178–33187.
22. Tang, C., Liu, Y., Kessler, P. S., Vaughan, A. M., & Oram, J. F. (2009). The macrophage cholesterol exporter ABCA1 functions as an anti-inflammatory receptor. *Journal of Biological Chemistry, 47*, 32336–32343.
23. Richmond, T. D., Chohan, M., & Barber, D. L. (2005). Turning cells red: signal transduction mediated by erythropoietin. *Trends in Cell Biology, 15*, 146–155.
24. Zannis, V. I., Lees, A. M., Lees, R. S., & Breslow, J. L. (1982). Abnormal apoprotein A-I isoprotein composition in patients with Tangier disease. *Journal of Biological Chemistry, 257*, 4978–4986.
25. Gordon, J. I., Sims, H. F., Lentz, S. R., Edelstein, C., Scanu, A. M., & Strauss, A. W. (1983). Proteolytic processing of human preproapolipoprotein A-I. A proposed defect in the conversion of pro A-I to A-I in Tangier's disease. *Journal of Biological Chemistry, 258*, 4037–4044.
26. Schmitz, G., Assmann, G., Rall, S. C., Jr., & Mahley, R. W. (1983). Tangier disease: defective recombination of a specific Tangier apolipoprotein A-I isoform (pro-apo A-i) with high density lipoproteins. *Proceedings of the National Academy of Sciences of the United States of America, 80*, 6081–6085.
27. Reinhart, W. H., Gossi, U., Butikofer, P., et al. (1989). Haemolytic anaemia in analpha-lipoproteinaemia (Tangier disease): morphological, biochemical, and biophysical properties of the red blood cell. *British Journal Haematology, 72*, 272–277.
28. Sasaki, J., Waterman, M. R., & Cottam, G. L. (1986). Decreased apolipoprotein A-I and B content in plasma of individuals with sickle cell anemia. *Clinical Chemistry, 32*, 226–227.
29. Ginsberg, H. N., Le, N. A., & Gilbert, H. S. (1986). Altered high density lipoprotein metabolism in patients with myeloproliferative disorders and hypocholesterolemia. *Metabolism, 35*, 878–882.

Gene therapy for oral squamous cell carcinoma with *IAI.3B* promoter-driven oncolytic adenovirus-infected carrier cells

TING ZHANG[1], KATSUYUKI HAMADA[2], MASAMITSU HYODO[3], HIROSHI ITOH[4], KENZABURO TANI[5], HIROYUKI GODA[1], KOH-ICHI NAKASHIRO[1] and HIROYUKI HAMAKAWA[1]

Departments of [1]Oral and Maxillofacial Surgery, and [2]Obstetrics and Gynecology, School of Medicine, Ehime University, Shitsukawa, Toon, Ehime 791-0295; [3]Department of Otolaryngology, Kochi Medical School, Kohasu, Okoh-cho, Nankoku, Kochi 783-8505; [4]Animal Medical Center, Tokyo University of Agriculture and Technology, 3-5-8 Saiwai-cho, Fuchu-shi, Tokyo 183-8509; [5]Department of Advanced Molecular and Cell Therapy, Kyushu University Hospital, Kyushu University, Maidashi, Higashi-ku, Fukuoka 812-8581, Japan

Received September 29, 2010; Accepted November 26, 2010

DOI: 10.3892/or.2010.1130

Abstract. Although replication-competent oncolytic viral vectors have been developed to improve antitumor activity, the generation of high titers of neutralizing antibodies inhibits repetitive viral infection. Many studies have reported that oncolytic virus-infected carrier cells can overcome this viral induced immunogenicity. However, the effects of oncolytic virus-infected carrier cells in human oral squamous cell carcinoma (OSCC) have not yet been examined. In the present study, simulating the clinical trial, we examined the antitumor activity of carrier cells infected with oncolytic adenovirus AdE3-*IAI.3B* in human OSCC. *IAI.3B* was highly activated in OSCC cells but not in normal cells. AdE3-*IAI.3B* killed OSCC cells *in vitro* but not normal cells. AdE3-*IAI.3B*-infected A549 carrier cells eradicated OSCC GFP-SAS tumors in nude mice. Anti-adenovirus neutralizing antibodies completely blocked the antitumor effect of AdE3-*IAI.3B* but did not block that of carrier cells. After the induction of anti-adenoviral CTL responses by immunization of adenovirus, administration of carrier cells induced complete regression of murine squamous cell carcinoma SCC7 tumors. Adenovirus-*GM-CSF* augmented the antitumor effect of carrier cells. The *IAI.3B*-driven oncolytic adenovirus-infected carrier cell system might prove useful in the treatment of OSCC and clinical trials of it should be conducted in the near future.

Correspondence to: Dr Katsuyuki Hamada, Department of Obstetrics and Gynecology, School of Medicine, Ehime University, Shitsukawa, Toon, Ehime 791-0295, Japan
E-mail: hamakatu@m.ehime-u.ac.jp

Key words: *IAI.3B*, oral squamous cell carcinoma, oncolytic adenovirus, carrier cell, promoter

Introduction

More than 700 clinical trials of cancer gene therapy have been conducted in the USA, but encouraging clinical results have yet to be obtained. Recently, replication-competent oncolytic viral vectors have been developed to improve antitumor activity. However, there remain two major concerns with the use of these oncolytic vectors: frequent relapse of tumors despite temporary inhibition of tumor progression (1), and the generation of high titers of neutralizing antibodies which subsequently inhibit repetitive viral infection (2). Repetitive infection is difficult to achieve, although anti-CD3 antibody (2), polyethylene glycol (3), liposome (4), etoposide (5), and cyclophosphamide (6) have been tested in attempts to overcome the humoral immune responses to viral vectors.

Many studies of oncolytic vector-infected carrier cells have been reported, including intraperitoneal injection of PA-1 ovarian carcinoma cells infected with an oncolytic HSV-1 to treat intraperitoneal ovarian carcinoma xenografts (7), intravenous injection of MDA-MG-231 breast carcinoma cells infected with wild-type adenovirus to treat lung metastatic foci of breast carcinoma xenografts (8), intravenous injection of mesenchymal stem cells infected with oncolytic adenovirus to treat lung and breast tumor xenografts (9), intravenous injection of myeloma cells infected with oncolytic measles, vaccinia, vesicular stomatitis virus, and coxsackievirus A21 to treat orthotopic myeloma xenografts (10), intravenous injection of cytokine-induced killer cells infected with modified vaccinia virus to treat intraperitoneal ovarian tumors and subcutaneous breast tumors in syngeneic mice (11), intravenous injection of rat hepatoma cells infected with oncolytic parvovirus to treat lung metastatic foci of syngeneic rat hepatoma tumors (12), intravenous injection of CT26 tumor cells infected with oncolytic vesicular stomatitis virus to treat lung metastatic foci of syngeneic mouse CT26 colon tumors (13), intravenous injection of autologous $CD8^+$ lymphocytes infected with oncolytic vesicular stomatitis virus to treat lymphnode metastatic foci of syngeneic mouse melanoma tumors (14), and

intratumoral injection of A549 tumor cells infected with oncolytic adenovirus to treat syngeneic mouse ovarian tumors (15). These carrier cell treatments have yielded significant antitumor effects in syngeneic and non-syngeneic mouse tumors and completely overcome the inhibition of virus infection by antiviral antibody production (13,15).

The *IAI.3B* gene was originally isolated using polyclonal antibodies to a high-molecular-weight fraction derived from ovarian carcinoma (16). The promoter activity of the *IAI.3B* gene is specific for ovarian carcinoma, and an oncolytic adenovirus termed AdE3-*IAI.3B*, in which the *E1A* gene is under the control of the human *IAI.3B* promoter, replicates as efficiently as the wild-type adenovirus in ovarian carcinoma cells but causes regrowth following temporary inhibition of growth of ovarian carcinoma cell tumors (17). However, the promoter activity of the *IAI.3B* and the effects of AdE3-*IAI.3B* in human oral squamous cell carcinoma (OSCC) have not yet been examined. In a previous study (15), human non-small cell lung cancer A549 carrier cells were infected with AdE3-*IAI.3B* and the adenoviral particle-containing cell fragments derived from the carrier cells were engulfed by target cancer cells. This non-receptor-mediated adenoviral transfection system circumvented neutralization by anti-adenovirus antibodies and enhanced antitumor activity after the induction of anti-adenoviral CTL responses by preimmunization with adenovirus in syngeneic mice, and an antitumoral immune response was then induced. Combination with GM-CSF augments the antitumor effects of carrier cells and induces complete tumor reduction (15). In the present study, we examined the promoter activity of *IAI.3B*, the antitumor activity of AdE3-*IAI.3B*, and the antitumor activity of carrier cells infected with AdE3-*IAI.3B* in OSCC.

Materials and methods

Cell lines and culture conditions. Human non-small cell lung cancer A549, human cervical squamous cell carcinoma SKGIIIa, human OSCC HSC-2, HSC-3 and HSC-4, human skin squamous cell carcinoma HSC-5, and human breast carcinoma MCF-7 cells were obtained from the Japanese Collection of Research Bioresources Cell Bank (Osaka, Japan). The human ovarian clear cell carcinoma KK and human ovarian adenocarcinoma KF cells were gifts from Dr Y. Kikuchi, National Defense Medical College, Tokorozawa, Japan. Human ovarian adenocarcinomas OCC1, 420, OVCAR3, 429, and HEY cells were obtained from Dr G. Mills and murine squamous cell carcinoma SCC7 from Dr L. Milas (The University of Texas, M.D. Anderson Cancer Center, TX, USA). Normal human keratinocyte K42 and normal human fibroblast F27 cells were established by Dr K. Hashimoto, Ehime University, Japan. Normal human ovarian fibroblast NOE-1 cells were established in our laboratory. Human umbilical vein endothelial HUVECs were obtained from Cambrex Bio Science Walkersville Inc. (Walkersville, MD). Human OSCC GFP-SAS was established by S. Shintani (Showa University, Tokyo, Japan). Human OSCC Ca9-22 was obtained from the Cell Resource Center for Biomedical Research (Institute of Development, Aging and Cancer, Tohoku University). Human cervical squamous cell carcinoma HT-III and CaSki cells, human cervical adenocarcinoma HeLa, human colorectal adenocarcinoma HT-29, and human pancreas carcinoma PANC-1 cells were obtained from the American Type Culture Collection (Rockville, MD).

Cells were maintained in a humidified 5% CO_2/95% air incubator at 37°C. All cell lines except K42 and HUVECs were grown in RPMI medium supplemented with 10% heat-inactivated fetal bovine serum. K42 cells were grown in MCDB153 (Nissui Co., Tokyo, Japan) with bovine hypothalamus extract. HUVEC cells were grown in EBM-2 (Cambrex, MD).

Construction of the AdE3-IAI.3B vector. The pXC1 plasmid has adenovirus 5 sequences from nt 22 to nt 5790 containing the *E1* gene (Microbix Biosystems Inc., Toronto, Canada). A unique *Age*I site was introduced to generate the plasmid pXC1-*Age*I. The *IAI.3B* promoter was ligated to pXC1-*Age*I plasmid to obtain pXC1-*IAI.3B*. To construct the AdE3-*IAI.3B* virus, homologous recombination was performed between pXC1-*IAI.3B* plasmid and the right-hand side of pBHGE3 adenovirus DNA containing the *E3* region in 293 cells by a standard technique (17). To construct the wild-type adenovirus AdE3, homologous recombination was performed between pXC1 and pBHGE3 in 293 cells. The replication-defective *E1*-deleted Ad-*ß-gal* virus was used as control adenovirus. All viruses were purified with double Cesium Chloride gradients using standard methods, and titered with standard spectrophotometry and plaque assay (17). AxCA*mGM-CSF* was obtained from RIKEN Bioresource Center (Tsukuba, Japan).

Real-time quantitative RT-PCR. RNA samples (100 ng) were used in RT and real-time PCR for RNA expression studies. Reverse transcriptase and real-time PCR reactions were carried out with the ABI prism 7700 sequence detection system (Applied Biosystems, Foster City, CA) in a total volume of 50 μl that contained TaqMan one step RT-PCR master mix (Applied Biosystems), 0.3 μM of each forward and reverse primer, and 0.21 μM of MGB probe. The forward and reverse primer and MGB probe for *IAI.3B* were respectively 5'-CCACTTGTTCCATGTGACACAGA-3', 5'-CCGTTTCGTTAACCACTTGTTCTC-3' and 5'-AAGACAAGCCCCCAGACTGGTTCACAAG-3', respectively. The reaction was performed with the following thermal cycling method: 30 min at 48°C for reverse transcription, 5 min at 95°C for AmpliTaq Gold activation, 15 sec at 95°C and 60 sec at 60°C for 40 cycles. GAPDH was chosen as a housekeeping gene to be tested as an endogenous control.

Assay for promoter activity. *IAI.3B* promoter fragment was inserted into the luciferase reporter vector PicaGene Basic, a promoterless and enhancerless vector (Toyo INK MFG Co., Tokyo, Japan). The sequence of the insert was confirmed with an ABI PRISM 310 Genetic Analyzer (Applied Biosystems). Construct containing *IAI.3B* promoter sequence was fused to the *Luciferase* gene which was transfected into cells in the presence of Lipofectamine transfection reagent (Invitrogen, Carisbad, CA) according to the protocol recommended by the manufacturer. Briefly, $1x10^5$ cells seeded in a 12-well culture dish were exposed to transfection mixtures containing 1 μg of luciferase reporter plasmids and 0.2 μg

of *prenilla luciferase-herpes simplex virus thymidine kinase* promoter control vector (Promega, Madison, WI) at 37°C for 48 h. Dual luciferase assays were performed according to the manufacturer's protocol (Promega).

Crystal violet assay. Cells were plated at a density of 2000 cells/well in 96-well plates. Cells were infected with AdE3-*IAI.3B*, AdE3, and co-cultured with AdE3-*IAI.3B*- and AdE3-infected carrier cells with or without high titer (x6,000) of anti-adenovirus antibodies (Takeda Pharmaceutical, Tokyo, Japan). After 5 days, cells were fixed and stained with 0.5% crystal violet in 50% methanol for 1 h at room temperature, washed with water, and air-dried, and each well was scanned with a spectrophotometric microplate reader (Immuno Mini, NJ-2300, Nalge Nunc International K.K., Tokyo, Japan) at the wavelength of 540 nm. The 50% growth inhibitory concentration (IC_{50}) was determined.

Inhibition of subcutaneous tumor growth in vivo. To determine the inhibition of xenograftic subcutaneous tumor growth, AdE3-*IAI.3B* was injected into subcutaneous tumors in female nude (*nu/nu*) mice (CLEA Japan Inc., Tokyo). In brief, $1x10^7$ GFP-SAS cells in 100 μl of RPMI were injected into the left posterior flank of each mouse through an insulin syringe with a 27 1/2-gauge needle. In each group 5-10 animals were used. After 20-30 days, small (4-5 mm) or large (8-10 mm) tumors were established. Then 100 μl of AdE3-*IAI.3B* ($1x10^{10}$ PFU, plaque forming units), AdE3 ($1x10^{10}$ PFU), Ad-*ß-gal* ($1x10^{10}$ PFU), medium alone, or A549 carrier cells infected with AdE3-*IAI.3B* at 200 MOI (multiplicity of infection) were injected intratumorally on days 0, 1, 2, 3, 4 and 5. The tumors were measured every 2 days with calipers to determine two perpendicular diameters. Tumor volume was calculated by assuming a spherical shape, with average tumor diameter calculated as the square root of the product of cross-sectional diameters.

To determine inhibition of syngeneic subcutaneous tumor growth, murine SCC7 cells ($1x10^6$) were injected into the left thigh of female C3H mice (CLEA) and AdE3-*IAI.3B*-infected A549 carrier cells were injected into subcutaneous tumors. Five to ten animals were used for each group. Medium alone, AdE3-*IAI.3B* ($1x10^{10}$ PFU), or A549 carrier cells ($5x10^6$) infected with AdE3-*IAI.3B* at 200 MOI with or without AxCA*mGM-CSF* at 10 MOI were injected into the tumors on days 0, 1, and 2. Mice were preimmunized with Ad-*ß-gal* ($1x10^{10}$ PFU) 21 days before the inoculation of SCCA7 cells. The animal studies were approved by the Ehime University Review Board.

Statistical analyses. Values are the mean ± SD, and were examined with the unpaired t-test, Cochran-Cox test, Welch test, and regression analysis. Survival data were plotted on Kaplan-Meier curves, and examined with the log-rank test using the LIFETEST procedure. Findings of $P<0.05$ were considered significant.

Results

mRNA levels of IAI.3B in OSCC cells. To examine the mRNA levels of *IAI.3B* in OSCC cells, one-step real-time RT-PCR was performed using MGB probe. The mRNA levels of *IAI.3B* in OSCC cells were not significantly different from those in ovarian, cervical and other cancer cells but 6 times higher than those in normal cells (Fig. 1A).

Transcriptional activities of IAI.3B in OSCC cells. To examine the transcriptional activities of *IAI.3B* in OSCC cells, transient expression assays were performed. Luciferase reporter plasmid containing the 5'-flanking regions of 1875 bp upstream from the transcriptional start site of the *IAI.3B* gene was constructed and transfected into each cell, and cell lysates were tested in luciferase assays. Fig. 1B demonstrates the transcriptional activities in each cell. The promoter activity of *IAI.3B* in OSCC cells was not significantly different from those in ovarian, cervical and other cancer cells but 36 times higher than those in normal cells.

Transcriptionally targeted AdE3-IAI.3B has potent anti-proliferative effects in OSCC, ovarian, cervical, and other cancer cells but not in normal cells. To determine the most appropriate infection condition, AdE3-*IAI.3B* was infected in A549 cells at various MOIs and infection times. A549 carrier cells infected with AdE3-*IAI.3B* at 200 MOI for 33-48 h exhibited the most potent anti-proliferative effect on HEY cells in the presence of antiadenovirus antibodies (Fig. 2A and B). Furthermore, 12-36 h of infection induced the least injury of carrier cells infected with AdE3-*IAI.3B* at 200 MOI (Fig. 2C). Therefore, 200 MOI for 33-36 h was considered the best set of conditions for infection of carrier cells. More than 48 h of infection induced severe injury in carrier cells infected with AdE3-*IAI.3B* at 200 MOI (Fig. 2C). Furthermore, 33 h of infection was adopted as the infection time, since it is more convenient than 36 h.

To estimate the potential of *IAI.3B* promoter for use in gene therapy of OSCC, AdE3-*IAI.3B* was transfected into each cell line. Fig. 3A shows the growth-inhibitory effects (IC_{50}) of AdE3-*IAI.3B* in various types of cell lines. The IC_{50} of AdE3 did not differ significantly among OSCC, ovarian, cervical, other cancer cells, and normal cells. AdE3-*IAI.3B* did not kill normal cells but significantly suppressed the growth of OSCC, ovarian, cervical and other cancer cells. Fig. 3B shows the growth-inhibitory effects (IC_{50}) of AdE3-*IAI.3B*-infected carrier cells in various types of cell lines. The IC_{50} of AdE3-infected carrier cells did not differ significantly among OSCC, ovarian, cervical, other cancer cells, and normal cells. However, AdE3-*IAI.3B*-infected carrier cells did not kill normal cells but significantly suppressed the growth of OSCC, ovarian, cervical, and other cancer cells.

AdE3-IAI.3B- and AdE3-IAI.3B-infected A549 carrier cells suppress subcutaneous tumor growth of OSCC, respectively, in nude and syngeneic mice. To evaluate the antitumor effect of AdE3-*IAI.3B* in small tumors, subcutaneous xenograft tumors, 4-5 mm diameter were established in the left flanks of nude mice using GFP-SAS OSCC cells. By 12 days, we observed significant reduction in tumor size in the AdE3-*IAI.3B*- and AdE3-treated groups compared with the medium-alone- and Ad-*ß-gal*-treated groups in the GFP-SAS tumor models. By 30 days, complete tumor regression was transiently

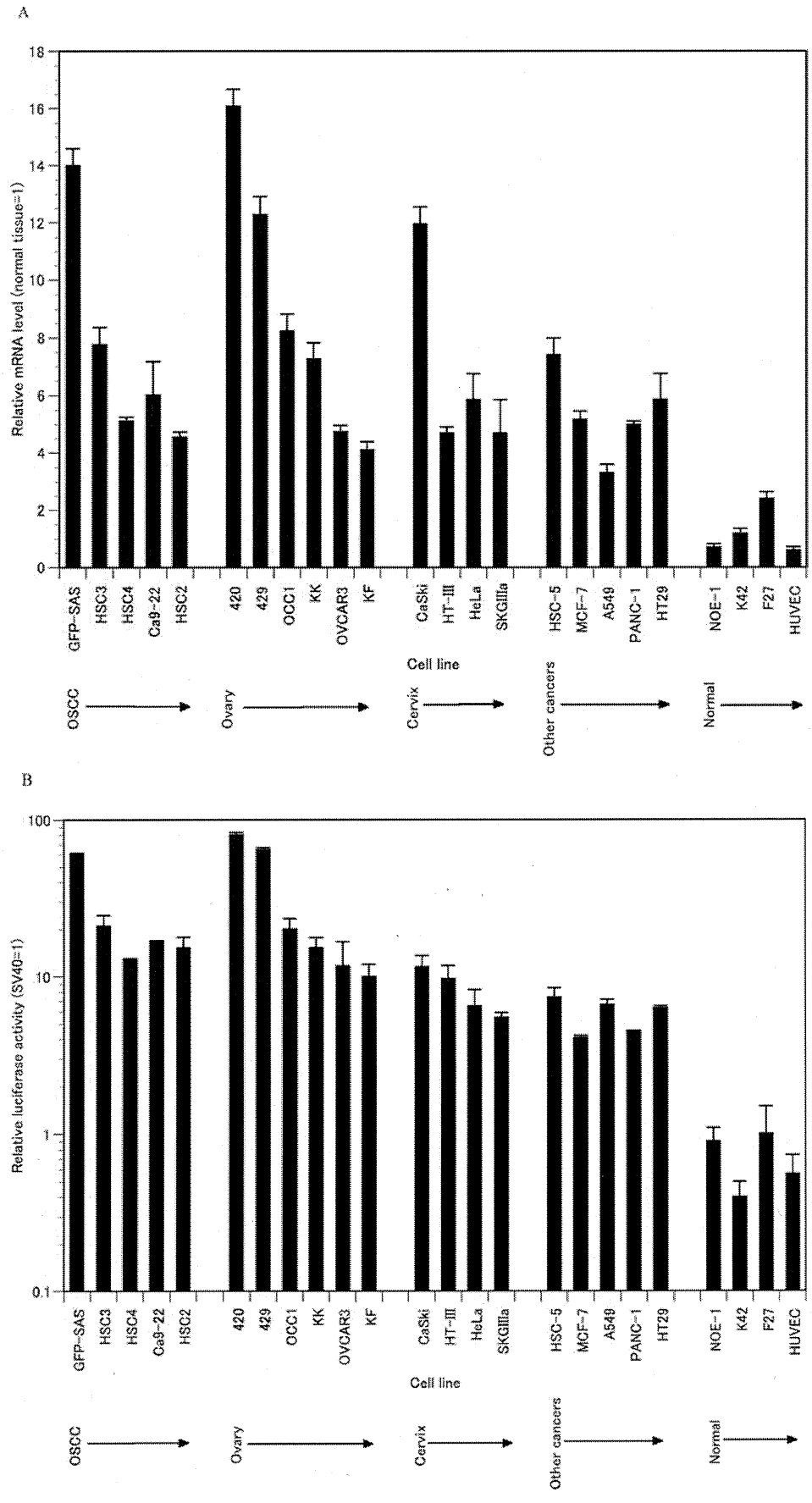

Figure 1. (A) *IAI.3B* mRNA levels determined by real-time RT-PCR and (B) transcriptional activity of *IAI.3B* promoter in head and neck squamous cell, ovarian, cervical, other cancer and normal cells. mRNA and luciferase activities were plotted as ratios to those in the normal tissue and the control plasmid (pGV-*SV40*) driven by the *SV40* enhancer/promoter, respectively. Bars, SD.

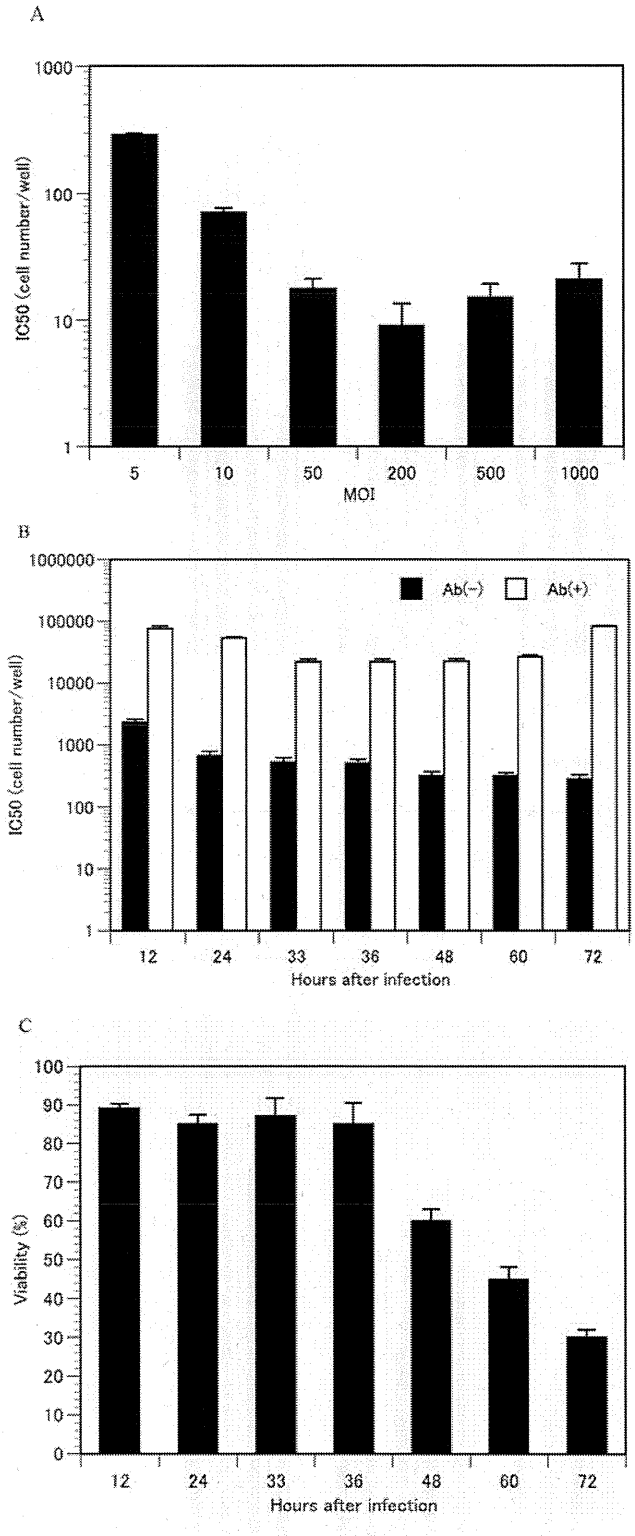

Figure 2. (A) The growth-inhibitory effects (IC_{50}) of AdE3-*IAI.3B* at various MOIs with anti-adenovirus neutralizing antibodies. (B) The growth-inhibitory effects (IC_{50}) of AdE3-*IAI.3B*-infected carrier cells at various infection times with or without anti-adenovirus neutralizing antibodies (Ab). (C) The viability of A549 carrier cells infected with AdE3-*IAI.3B* at various infection times. Bars, SD.

observed in the AdE3-*IAI.3B*- and AdE3-treated groups, though all tumors regrew by 60 days (Fig. 4A). To evaluate the antitumor effect of AdE3-*IAI.3B* in large tumors, xenograftic subcutaneous tumors with 8-10-mm diameter were established in the left flanks of nude mice using GFP-SAS. By 20-50 days after initiation of intratumoral injections, AdE3-*IAI.3B* had significantly repressed the growth of GFP-SAS tumors, but AdE3-*IAI.3B*-injected tumors regrew 60 days after the initiation of treatment, to an extent not significantly different from the medium-treated control and Ad-*β-gal* (Fig. 4B). In contrast, carrier cells infected with AdE3-*IAI.3B* completely suppressed the growth of GFP-SAS tumors 40 days after initiation of treatment and induced complete tumor regression.

To evaluate the antitumor effects of AdE3-*IAI.3B* after immunization in an immunocompetent syngeneic mouse model, C3H mice were immunized with Ad-*β-gal* and subcutaneous tumors with 5-8-mm diameter were established in the left thigh of C3H female mice using SCC7 cells (Fig. 4C). Survival of control mice was not significantly different from that of the mice treated with AdE3-*IAI.3B* alone. The survival of mice treated with A549 carrier cells infected with AdE3-*IAI.3B* was significantly longer than those of the mice treated with medium control or AdE3-*IAI.3B*. Furthermore, simultaneous infection with AxCA*mGM-CSF* augmented the antitumor effect of A549 carrier cells infected with AdE3-*IAI.3B* and induced complete elimination of tumor in all treated mice. Mice that exhibited complete tumor regression were resistant to subsequent inoculation of SCC7 cells.

Discussion

The *IAI.3B* promoter-introduced replication-competent oncolytic adenovirus AdE3-*IAI.3B* replicates as efficiently as wild-type adenovirus in human OSCC, human ovarian carcinoma, human cervical carcinoma, and other cancer cells expressing high levels of *IAI.3B*, but does not in normal cells expressing low levels of *IAI.3B* (17). However, intratumoral administration of AdE3-*IAI.3B* alone yielded no prominent therapeutic effects in nude mice bearing large xenografts; nevertheless, injection of AdE3-*IAI.3B*-infected A549 carrier cells into the tumors produced significant antitumor effects. The antitumor effect of carrier cells in nude mice could be due to increases in local retention time and local concentration of AdE3-*IAI.3B* by delivery from carrier cells. Direct intratumoral administration of oncolytic adenoviruses such as ONYX-015 did not prevent the recurrence of treated tumors, although ONYX-015 transiently eradicated tumors in nude mice (1). More than 90% of intratumorally injected adenoviruses in nude mice migrate into the systemic circulation and accumulate in the liver (15). Therefore, oncolytic adenovirus itself is unable to induce complete tumor regression in nude mice, though oncolytic adenovirus-infected carrier cells are able to.

Treatment with PEGylation (3), liposome-encapsulation (4), etoposide (5) and cyclophosphamide (6) decreased the titer of neutralizing antibodies against adenoviruses and yielded partial recovery of adenoviral infectivity in target cells on the second injection. However, such modifications were ineffective in the case of third or later injections, due to the increase in anti-adenovirus antibody titers, and therefore,

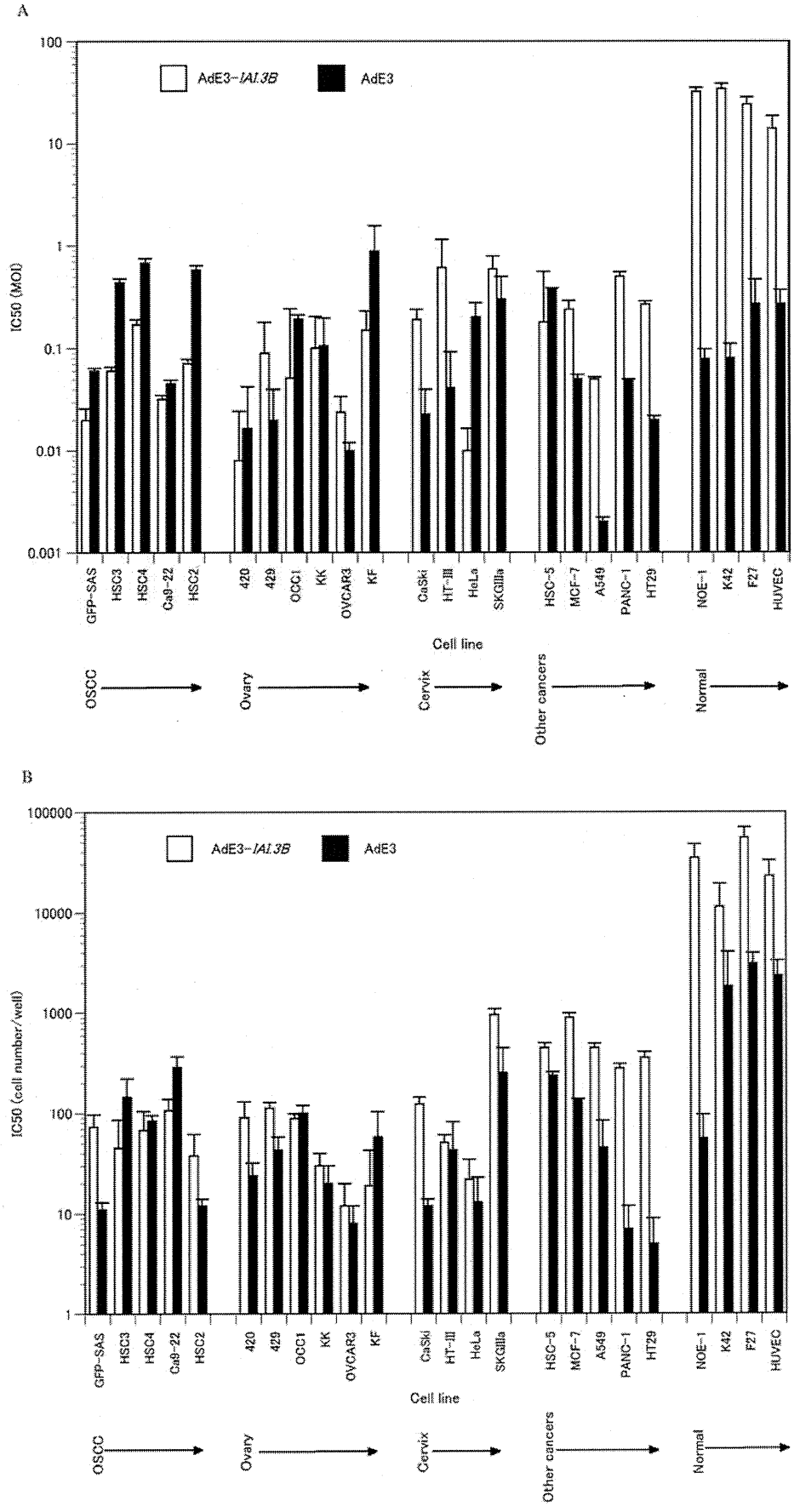

Figure 3. (A) The growth-inhibitory effects (IC_{50}) of AdE3-*IAI.3B* and AdE3 and (B) the IC_{50} of AdE3-*IAI.3B*- and AdE3-infected A549 carrier cells in OSCC, ovarian, cervical, other cancer and normal cells without anti-adenovirus neutralizing antibodies. Bars, SD.

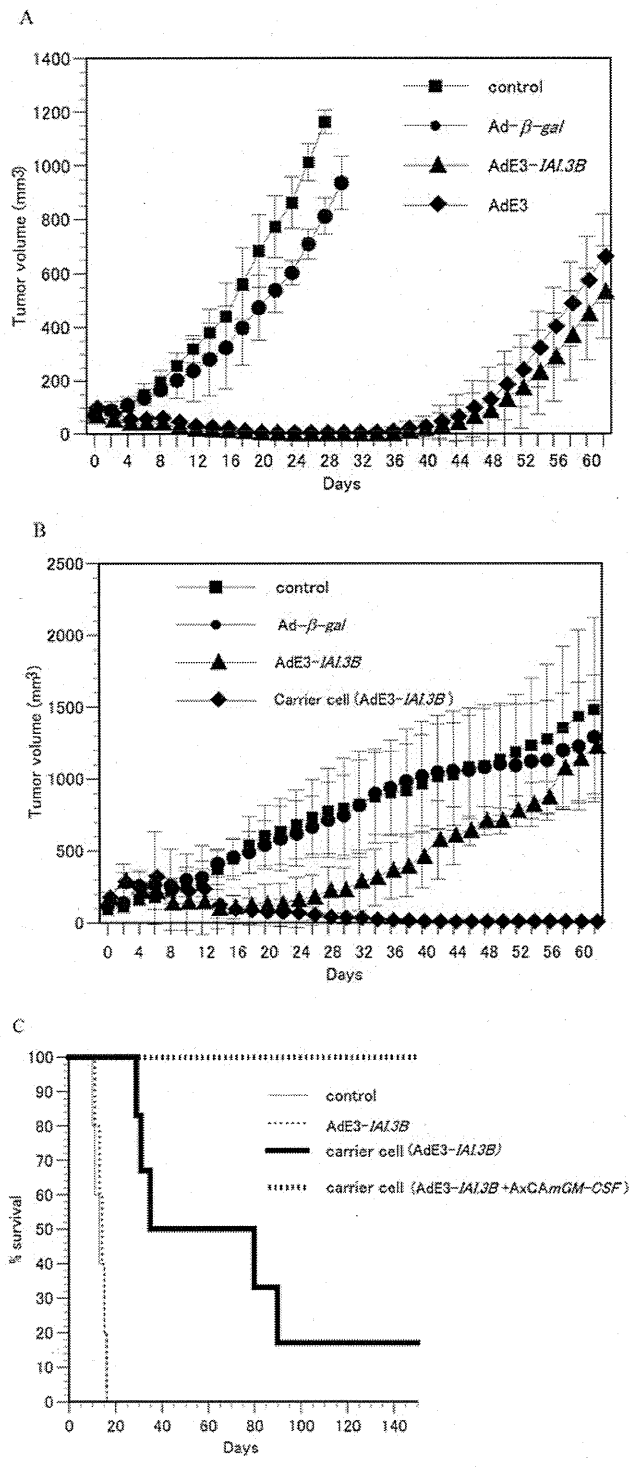

Figure 4. (A) The antitumor effects of AdE3-*IAI.3B* in subcutaneous OSCC GFP-SAS small (4-5 mm) tumors in nude mice. (B) The antitumor effects of A549 carrier cells infected with AdE3-*IAI.3B* in large GFP-SAS subcutaneous OSCC (8-10 mm) tumors in nude mice. (C) The antitumor effects of A549 carrier cells infected with AdE3-*IAI.3B* against subcutaneous syngeneic SCC7 tumors established in C3H mice after immunization. RPMI medium, Ad-*β-gal*, AdE3-*IAI.3B*, and A549 carrier cells infected with AdE3-*IAI.3B* with or without AxCA*mGM-CSF* were injected into each tumor. Bars, ±SD.

could not produce significant antitumor effects in immunocompetent animals. Moreover, murine cancer cells are resistant to replication-competent viral gene therapy because of their lower expression of adenoviral receptors (18). However, our carrier cell system completely eradicated murine tumors in syngeneic mice and produced significant antitumor effects despite high titers of anti-adenovirus antibodies.

Our previous study demonstrated that A549 carrier cells bearing oncolytic adenoviruses delivered adenoviral particles through their cell fragments to target cells (15). Engulfment of cell fragments was observed only in proliferative malignant cells and not in non-proliferative normal cells. Carrier cell-mediated adenoviral infection consequently produced CTL responses against adenoviruses. Furthermore, mice with complete tumor regression obtained protective immunity. It thus appears that the cell fragment-mediated transfer of adenovirus is independent of adenovirus receptors and is not blocked by anti-adenovirus antibodies. Many studies of oncolytic virus-infected carrier cell systems have been reported in oncolytic HSV-1 mutant-infected PA-1 cells (7), in modified vaccinia virus-infected cytokine-induced killer (CIK) cells (11), in oncolytic adenovirus-infected A549 cells (15), in vesicular stomatitis virus (VSV)-infected colon carcinoma cells (13), in nerve growth factor-transduced autologous fibroblasts (19), and in human interferon ß-transduced umbilical cord matrix stem cell (20). In this study, AdE3-*IAI.3B* selectively killed OSCC cells *in vitro* and *in vivo*. *IAI.3B* promoter-driven oncolytic virotherapy has not yet been reported in OSCC cells. The present study is the first report of *IAI.3B*-specific gene therapy for OSCC. Although clinical trials for adenovirus-p53 (21) and oncolytic adenovirus (22) for OSCC have been reported, the results of such clinical trials were clinically insufficient, since adenoviral infection was completely blocked by the production of anti-adenovirus neutralizing antibodies. This finding is identical to those for gene therapy with other viruses.

It has been reported that oncolytic virus-infected carrier cells overcome the viral-induced humoral immune response, the viral-induced cellular immune response kills virus-infected target cancer cells, and GM-CSF augments the anti-tumor effect of carrier cells (15). The present study also demonstrated that oncolytic adenovirus-infected A549 carrier cells induced elimination of tumor and adenovirus-*GM-CSF* augmented the anti-tumor effect of carrier cells, resulting in complete regression of tumor in mice. Furthermore, second challenge with syngeneic mouse squamous cell carcinoma was completely rejected by a specific antitumor response, also suggesting that the systemic tumor immune response induced by carrier cell treatment may cure not only the carrier cells-injected local tumors but also non-injected metastatic tumors. In conclusion, *IAI.3B* promoter-driven oncolytic adenovirus-infected carrier cells may cure OSCC and human clinical trials with AdE3-*IAI.3B*-infected carrier cells should be possible in the near future.

Acknowledgements

This study was supported by a grant from the Ministry of Education, Science, Sports and Culture, Japan and by the Integrated Center for Science, Ehime University. We thank K. Oka for preparing culture medium in this study.

References

1. Geoerger B, Grill J, Opolon P, *et al*: Oncolytic activity of the E1B-55kDa-deleted adenovirus ONYX-015 is independent of cellular p53 status in human malignant glioma xenografts. Cancer Res 62: 764-772, 2002.
2. DeMatteo RP, Yeh H, Friscia M, *et al*: Cellular immunity delimits adenoviral therapy strategies for the treatment of neoplastic diseases. Ann Sur Oncol 6: 88-94, 1999.
3. Mok H, Palmer DJ, Ng P and Barry MA: Evaluation of polyethylene glycol modification of first-generation and helper-dependent adenoviral vectors to reduce immune responses. Mol Ther 11: 66-79, 2005.
4. Yotnda P, Chen DH, Chiu W, *et al*: Bilamellar cationic liposomes protect adenovectors from preexisting humoral immune responses. Mol Ther 5: 233-241, 2002.
5. Bouvet M, Fang B, Ekmekcioglu S, *et al*: Suppression of the immune response to an adenovirus vector and enhancement of intratumoral transgene expression by low-dose etoposide. Gene Ther 5: 189-195, 1998.
6. Jooss K, Yang Y and Wilson JM: Cyclophosphamide diminishes inflammation and prolongs transgene expression following delivery of adenoviral vectors to mouse liver and lung. Hum Gene Ther 20: 1555-1566, 1996.
7. Coukos G, Makrigiannakis A, Kang EH, *et al*: Use of carrier cells to deliver a replication-selective herpes simplex virus-1 mutant for the intraperitoneal therapy of epithelial ovarian cancer. Clin Cancer Res 5: 1523-1537, 1999.
8. Garcia-Castro J, Martinez-Palacio J, Lillo R, *et al*: Tumor cells as cellular vehicles to deliver gene therapies to metastatic tumors. Cancer Gene Ther 12: 341-349, 2005.
9. Hakkrainen T, Sarkioja M, Lehenkari P, *et al*: Human mesenchymal stem cells lack tumor tropism but enhance the antitumor activity of oncolytic adenoviruses in orthotopic lung and breast tumors. Human Gene Ther 18: 627-641, 2007.
10. Munguia A, Ota T, Miest T and Russell SJ: Cell carriers to deliver oncolytic viruses to sites of myeloma tumor growth. Gene Ther 15: 797-806, 2008.
11. Thorne SH, Negrin RS and Contag CH: Synergistic antitumor effects of immune cell-viral biotherapy. Science 311: 1780-1784, 2006.
12. Raykov Z, Balboni G, Aprahamaian M and Rommelaere J: Carrier cell-mediated delivery of oncolytic parvoviruses for targeting metastases. Int J Cancer 109: 742-749, 2004.
13. Power AT, Wang J, Falls TJ, *et al*: Carrier cell-based delivery of an oncolytic virus circumvents antiviral immunity. Mol Ther 15: 123-130, 2007.
14. Qiao J, Kottke T, Willmon C, *et al*: Purging metastases in lymphoid organs using a combination of antigen-non-specific adoptive T cell therapy, oncolytic virotherapy and immunotherapy. Nat Med 14: 37-44, 2007.
15. Hamada K, Desaki J, Nakagawa K, Shirakawa T, Gotoh A and Tagawa M: Carrier cell-mediated infection of a replication-competent adenovirus for cancer gene therapy. Mol Ther 15: 1121-1128, 2007.
16. Campbell IG, Nicolai HM, Foulkes WD, *et al*: A novel gene encoding a B-box protein within the BRCA1 region at 17q21.1. Hum Mol Genet 3: 589-594, 1994.
17. Hamada K, Kohno S, Iwamoto M, *et al*: Identification of the human IAI.3B promoter element and its use in the construction of a replication-selective adenovirus for ovarian cancer therapy. Cancer Res 63: 2506-2512, 2003.
18. Miller CG, Krummenacher C, Eisenberg RJ, Cohen GH and Fraser NW: Development of a syngeneic murine B16 cell line-derived melanoma susceptible to destruction by neuroattenuated HSV-1. Mol Ther 3: 160-168, 2000.
19. Tuzynski MH, Thal L, Pay M, *et al*: A phase 1 clinical trial of nerve growth factor gene therapy for Alzheimer disease. Nat Med 11: 551-555, 2005.
20. Rachakatla RS, Marini F, Weiss ML, Tamura M and Troyer D: Development of human umbilical cord matrix stem cell-based gene therapy for experimental lung tumors. Cancer Gene Ther 14: 828-835, 2007.
21. Clayman GL, el-Naggar AK, Lippman SM, *et al*: Adenovirus-mediated p53 gene transfer in patients with advanced recurrent head and neck squamous cell carcinoma. J Clin Oncol 16: 2231-2231, 1998.
22. Nemunaitis J, Khuri F, Ganly I, *et al*: Phase II trial of intratumoral administration of ONYX-015, a replication-selective adenovirus, in patients with refractory head and neck cancer. J Clin Oncol 19: 289-298, 2001.